Effects of Atmospheric Pressure Loading on GPS Measurements

by

Jennifer L. Alltop
B.A. Astronomy-Physics
University of Virginia, 2001

SUBMITTED TO THE DEPARTMENT OF EARTH, ATMOSPHERIC AND PLANETARY SCIENCES IN PARTIAL FULFILLMENT OF THE REQUIREMENTS FOR THE DEGREE OF

MASTER OF SCIENCE IN GEOSYTEMS
PROFESSIONAL MASTER'S PROGRAM
AT THE
MASSACHUSETTS INSTITUTE OF TECHNOLOGY

JUNE 2002

Signature of author _____
Department of Earth, Atmospheric and Planetary Sciences
May 1, 2002

Certified by _____
Thomas A. Herring
Professor of Geophysics
Thesis Advisor

Accepted by _____
Ronald G. Prinn
Professor of Atmospheric Chemistry
Head, Department of Earth, Atmospheric, and Planetary Sciences

Abstract

With millimeter-level positioning capabilities, annual fluctuations in GPS height estimates can now be resolved. A likely explanation for these height variations is loading of the Earth's surface. We examine the relative contribution of atmospheric pressure loading to the total signal by modeling loads utilizing Farrell's elastic Green's functions. A focus on four permanent GPS sites provided insight on coastal and seasonal differences as well as the relative impact of atmospheric pressure loading on annual vertical displacements. Our findings suggest that accounting for the inverted barometer response [*Farrell,* 1972] of the ocean at coastal sites provides a better fit to GPS data. However, near restricted bodies of water we find that the non-inverted barometer fits better. We also found lower closer fits of the modeled pressure load to the GPS data during winter months than during the summer possibly due to larger pressure variations during the winter and/or mismodeling of tropospheric delay during summer months [*Herring,* 1990]. As for the contribution due to multiple sources of loading, in most cases, by adding an expected water load (from upper 2 meters of soil) to the atmospheric pressure load, a closer agreement to the GPS signal was found.

Chapter 1

Introduction

The latest GPS technology allows for millimeter-level positioning. With such high precision, we are capable of examining small scale loading effects on the Earth's surface. Loading phenomena are due to many sources such as ocean tides, atmospheric pressure, non-tidal oceanic loads, snow, and groundwater. We have reached a point with technology that millimeter-level variations of land height can conceivably be addressed and understood. In this study, we compare global GPS solutions to atmospheric pressure load models and water load data. The pressure load models use *Farrell's* [1972] elastic Green's functions as well as global meteorological data to predicted vertical surface variations.

We examine in detail global GPS solutions for four stations, picked for their location, analysis history, strength of annual signal, and the amount of data available. They are examined over the course of three years from 1999 to the beginning of 2002 using data from approximately 50 stations in the global solutions. The global network connects to form a polyhedron. The center of mass is the point at which the geocentric radii meet. Millimeter-level height resolutions can be found by removing a global translation from the daily solutions [*Blewitt et al.,* 1993]. With enough stations in the global solution individual station movements with respect to the average positions of all the stations are easy to discern.

We are interested in examining the contribution due to atmospheric pressure loading, the effect of the inverted barometer response at coastal versus inland sites, water load, and disagreements between analysis groups. This is the first study done using GPS data with high enough precision to view the periodic nature of the residual GPS signal. Past studies only knew they were decreasing the weighted root mean square scatter of the height residuals about a secular trend by accounting for the atmospheric pressure load contribution. These studies lacked the ability to resolve the signal [*van Dam and Herring*, 1994; *van Dam et al.,* 1994]. The statistical properties derived by *van Dam and Herring* [1994] have provided a basis for analysis in past studies. They considered the pressure loading correction equal to the sum of a loading term, σ_l^2, and a noise term, σ_w^2.

(1.1) $$< \sigma_{\delta b}^2 - \sigma_{\delta c}^2 > = \sigma_l^2 - \sigma_w^2$$

(1.2) $$\mathrm{var}(\sigma_{\delta b}^2 - \sigma_{\delta c}^2) = 4\sigma_v^2(\sigma_l^2 + \sigma_w^2)/(N-1)$$

where v is the noise in the GPS measurement. Equation 1 gives the expectation of the difference of the variance estimates of before, δb, and after, δc, and equation 2 gives the variance of the difference of the variance estimates. By the central limit theorem, the probability distribution of the variance difference can be approximated by a Gaussian distribution with expectation from equation 1 and variance from equation 2 for a sufficiently large N (> 30).

There is an agreement of numerical analyses in past studies that pressure loading can cause radial displacements on the Earth's surface of up to 25 mm [*Rabbel and Zschau,* 1985; *van Dam and Wahr,* 1987; *Manabe et al.,* 1991; *Rabbel and Schuh,* 1986]. We use two pressure load models, one incorporates the inverted barometer (IB) response of the oceans and the other is a rigid lid (no IB response) model. The inverted barometer response of the ocean to pressure changes is thought to be valid on timescales longer than a few days [*Wunsch,* 1972; *Ponte et al.,* 1991]. The two models are very close for inland sites where the IB response has a small or negligible impact on the loading. The difference in the models is large at coastal sites where the pressure load amplitude is smaller for the standard IB model. The ocean acts to dampen the vertical displacements seen at the coast.

Chapter 2

Farrell's Elastic Green's Functions

Modern GPS techniques allows for millimeter-precision positioning. Data collected over the past decade at sites around the world show periodic, centimeter-level signals in vertical displacement over time, which have come to be attributed to loading phenomena. Loading can take many forms including tidal, atmospheric pressure, non-tidal oceanic, and hydrologic loading. This paper focuses primarily on the nature of atmospheric pressure loading and its appearance in GPS data.

Mathematically, pressure loading can be described by Green's functions. A paper by *Farrell* [1972] goes into great detail about the use of Green's functions in describing mass loads on a spherical Earth. Green's functions are a generic way of solving partial differential equations and are widely used in models today to calculate the elastic response of the Earth's surface. Atmospheric pressure loading results in an elastic response unlike the slow visco-elastic response we see in post-glacial rebound. Farrell used the Gutenberg-Bullen A earth model to calculate Green's functions for one kilogram point mass loads on the Earth's surface at various distances from the loading point. The vertical displacement Green's function at a distance γ from the point mass load is

$$u(\gamma) = (a/m_e) \sum h_n P_n(\cos\gamma) \tag{2.1}$$

where a is the radius of the Earth, m_e is the Earth's mass, h_n is the load Love number and P_n is a Legendre polynomial. The horizontal displacement Green's function for the same load is

$$v(\gamma) = (a/m_e) \sum l_n \partial P_n(\cos\gamma) / \partial\gamma \tag{2.2}$$

where l_n is another Love number. The Love numbers or load-deformation coefficients [*Longman,* 1963] are different for different boundary conditions and are recalculated for different earth models. Equations 2.1 and 2.2 are the basis for Farrell's calculations and mathematical understanding of loading phenomena.

To learn more about the role that the upper region of the mantle plays in displacement, Farrell included two additional earth models in his calculations. He altered the upper 1000 km of the Guttenberg-Bullen A earth model by inserting oceanic and continental shield structures. The differences in the vertical displacement Green's function for the three models are illustrated in Figure 2.1. The most variation in the models is within one degree of the center of the load. The oceanic model shows greater values in this region. Although this is a small region of

disagreement in the models, it is where the greatest amount of vertical displacement is expected to take place. One degree is roughly 110 km on the Earth's surface. Figure 2.2 shows the radial profile of the expected surface displacements in mm/bar for each of the three models. We see the largest variation between the models within one degree of the center of the load as in Figure 2.1. The greatest difference is about 0.001 mm/bar between the models expectations. The G-B Model is therefore a very good approximation of all three. However the variability at small radii should be noted.

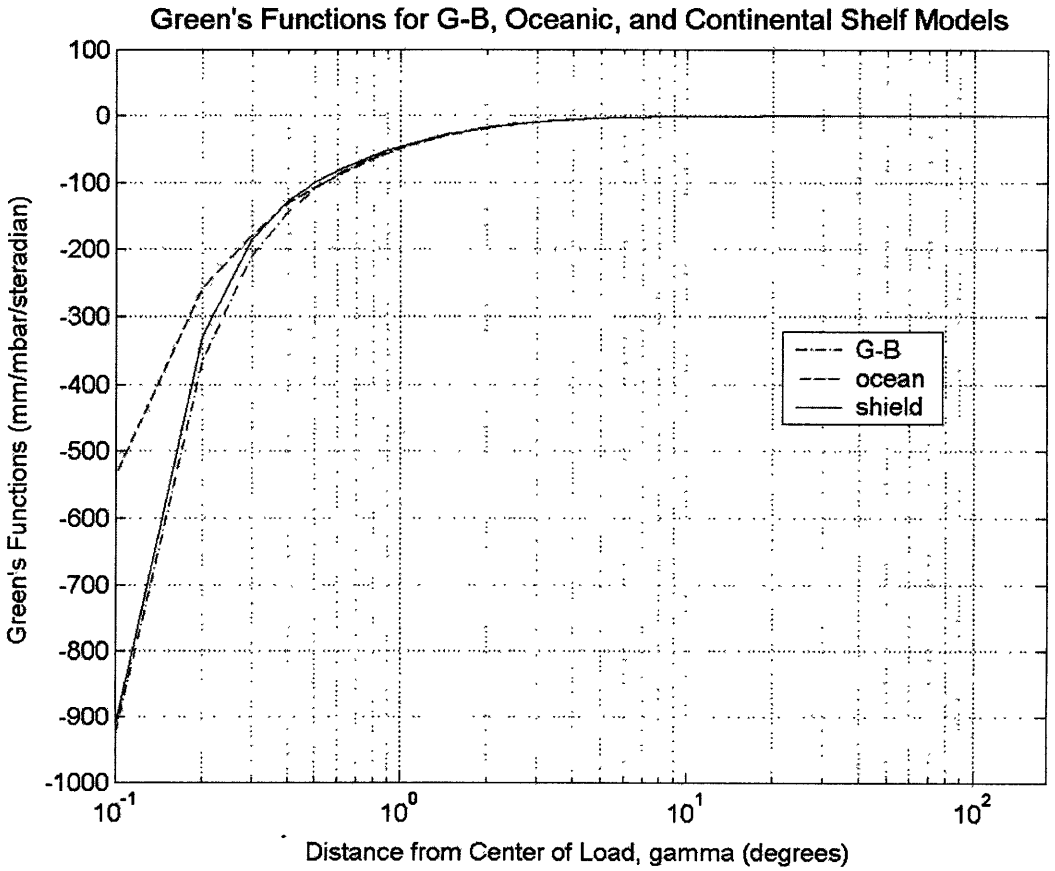

Figure 2.1 - Radial profile of Green's functions for three earth models.

The amount of displacement due to an atmospheric pressure load depends primarily on the size of the load, the distance from the center, latitude, and proximity to water. The loading effects become larger with increasing latitude (from equator to mid latitudes) due to increases in the scale of surface pressure variations [*van Dam and Wahr*, 1998]. The displacement is also

dependent on proximity to water due to the inverted barometer response of the oceans [*Wunsch,* 1972], which will be discussed in further detail in Chapter 4.

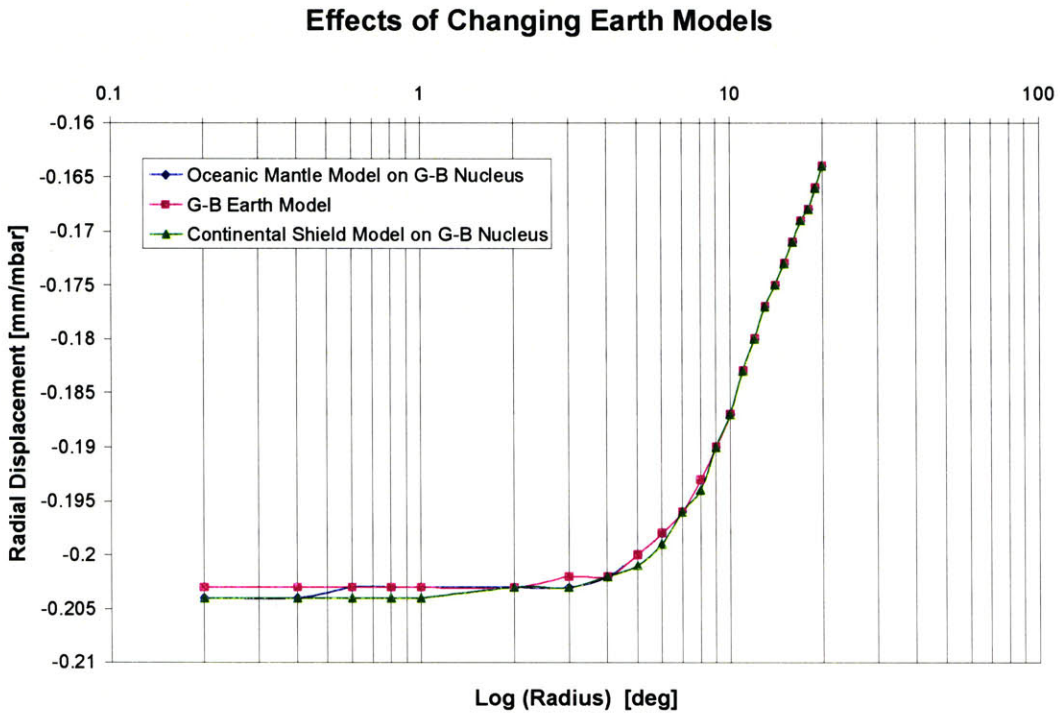

Figure 2.2 - Radial displacement vs. radius for three earth models for a 10 degree load. Differences appear at small radii.

Chapter 3

Modeling Disk Loads

Our model of pressure loading utilizes Farrell's elastic Green's functions as well as basic spherical trigonometry to derive radial and tangential displacements due to a given load on the Earth's surface. The model does a numerical integration to find the radial and tangential displacements at any point in a spherical cap for a load centered at the pole. The numerical integration consists of dividing the load into concentric circles and radial slices and then summing all of the areas of the individual boxes. We used a small concentric circle spacing of 0.01 degrees to better approximate the integral. The radial spacing is altered for each concentric circle to maintain boxes of similar areas for the entire load. Figures 3.1 and 3.2 show the radial displacements and tangential displacements respectively as a function of distance from the load center.

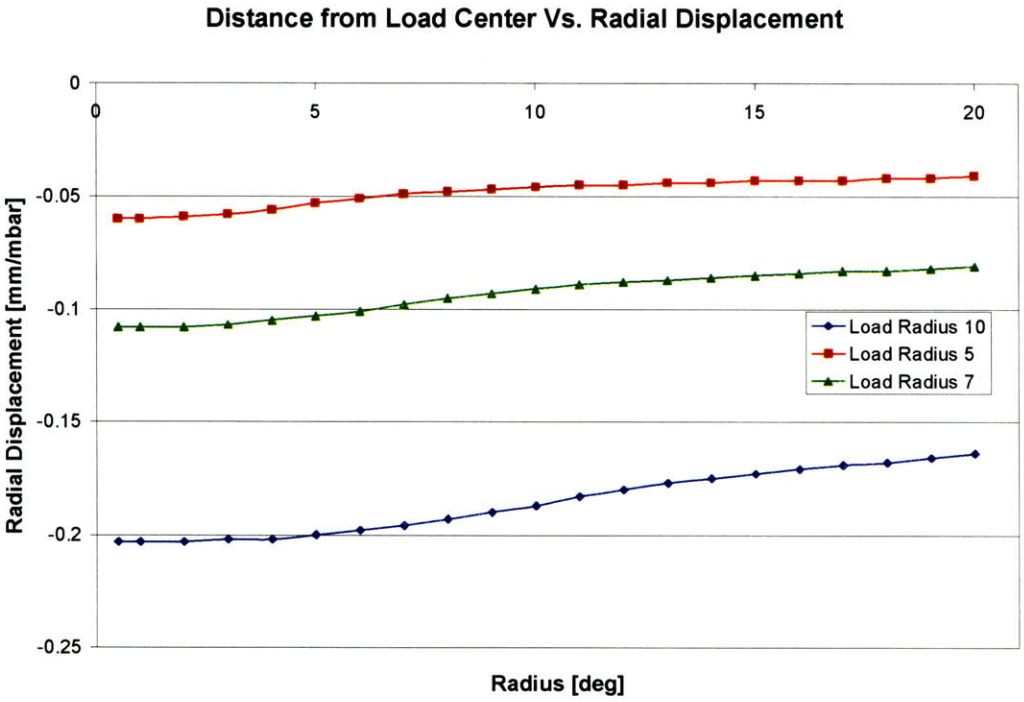

Figure 3.1 - The radial displacements in mm/mbar of loads of 5-, 7-, and 10-degree radius are displayed. These correspond to disks of 1100 km, 1500 km, and 2200 km. Displacements are shown with distance from center of load.

When a circular load is placed on a sphere the vertical displacement, radial displacement with respect to the sphere, is maximum at the center. The displacement decreases with distance

from the origin and is displaced even past the edge of the load. A loading occurrence due to a high-pressure front would cause a maximum vertical displacement at the center of the front and could still be noticed outside of the high-pressure region. The pressure front would also cause horizontal motion.

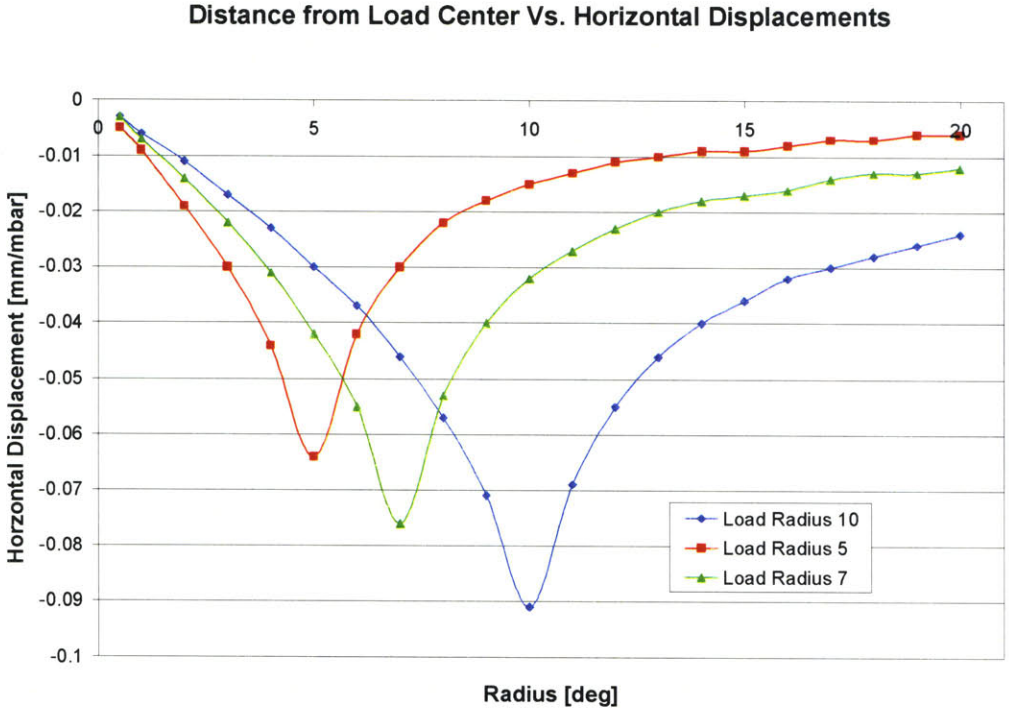

Figure 3.2 - The horizontal displacements in mm/mbar of loads of 5-, 7-, and 10-degree radius are displayed. Displacements are shown with distance from center of load.

The horizontal or tangential displacement works in just the opposite way of the radial displacement. In Figure 3.2 we see modeled displacements for three different size loads. The tangential displacement is zero at the center of the load and reaches its maximum at the edge. If we look at the ratio of the horizontal to vertical displacement we can see the relative influence of the two (See Figure 3.3).

As we see in Figures 3.1 and 3.2, the vertical displacement is a much larger effect. In Figure 3.3, the ratio goes to zero close to the center of the load showing the combined effect of the tangential displacement (numerator) being at a minimum and the radial displacement (denominator) being at a maximum. At the edge of the loads we see horizontal displacement is maximum. The radial displacement is maximum at the center of the load and minimum far

outside the load. We see as the loads get larger the vertical displacements get much bigger compared to the horizontal displacements. For large area loads there is a bigger difference between the two motions.

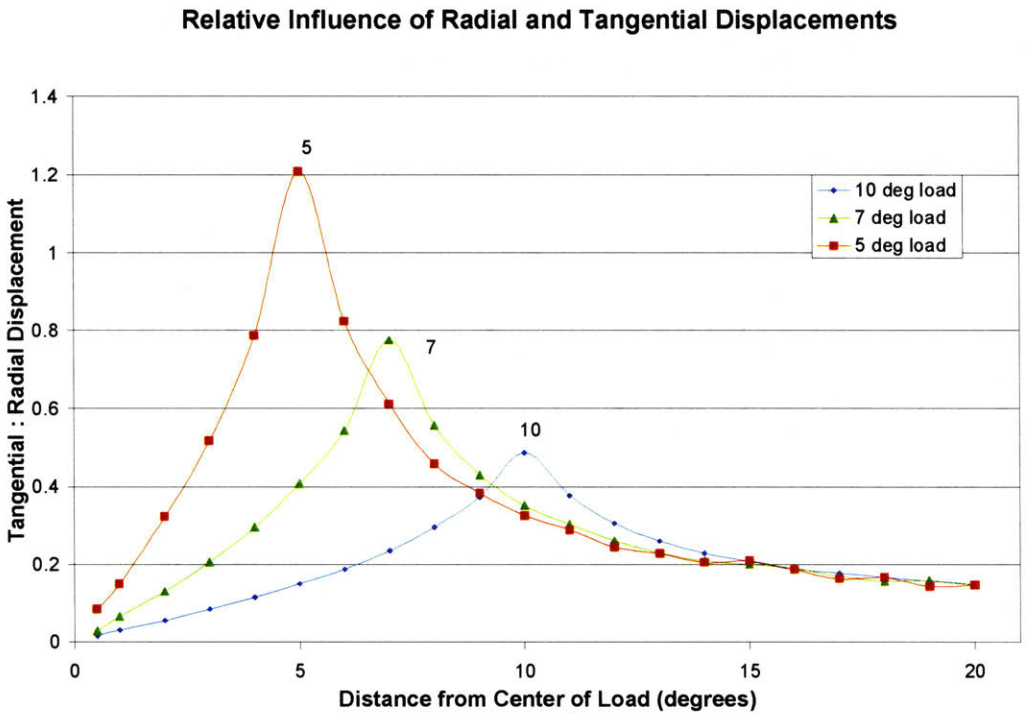

Figure 3.3 - Ratio of tangential to radial displacements for loads of 5-, 7-, and 10-degrees.

Figure 3.4 shows the sea level pressure anomaly between 1979 and 1995. The pressure cells can be very large so the vertical impact of such a loading event would be significantly larger than the horizontal impact. The 5, 7, and 10 degree loads correspond to disks of approximate radii 550 km, 780km, and 1100 km respectively. These are good representations of the size pressure cells we see in nature. The map shows a few cases of 5-mbar change over areas with 10-degree radii. If we use our 10-degree radius case discussed earlier we would expect to see a 1 mm vertical displacement at the center of the load and a 0.46 mm tangential displacement at the edge. With all of the GPS data being used to track small movements of faults in California, not taking atmospheric pressure loading into account when reducing data could result in misguided conclusions.

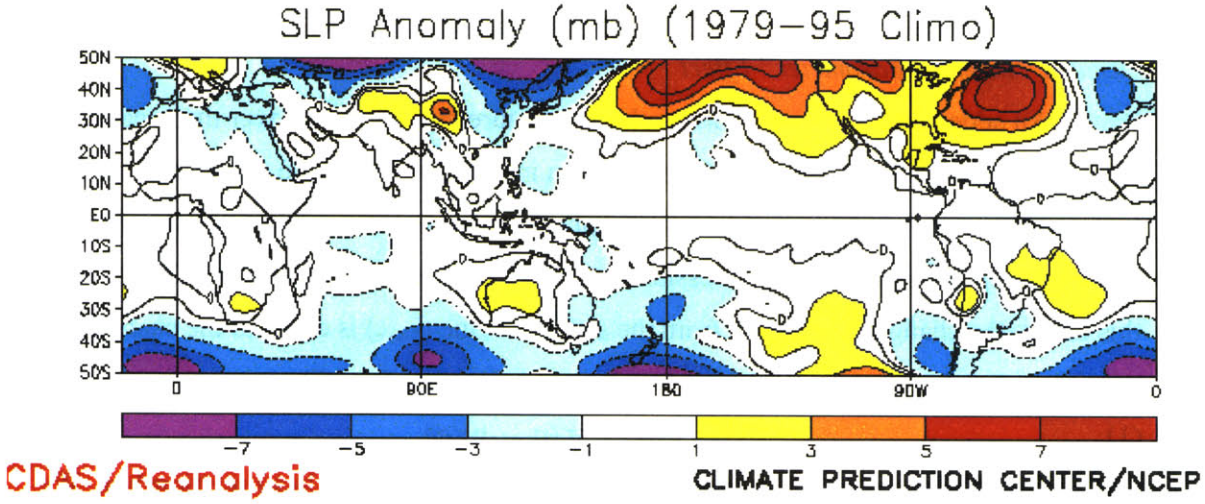

Figure 3.4 - Sea level pressure anomaly map, 1979 to 1995. Data from NCEP

Chapter 4

Oceanic "Inverted Barometer" Effect

An added complication to atmospheric pressure loading arises over the oceans. Under certain conditions, the ocean appears to act as an inverted barometer to changes in atmospheric surface pressure. A 1-mbar change in atmospheric surface pressure depresses the sea level by approximately 1 cm, the same depression a water barometer would measure [*Gill*, 1982]. With this effect, the change in sea level from the average value (L_{ave}) is equal to the change in pressure over the water density ($\rho \approx 10^3$ kg m^{-3}) multiplied by gravity (Eqn 1).

(1) $$L_{ave} - L = (p_{ave} - p)/\rho g$$

The average values are over the entire ocean so this is not a strictly local relationship. We assume the volume of the ocean stays constant over time. Therefore regional changes in pressure do not affect the total volume of the ocean.

Studies by *Wunsch* [1972], *Trupin and Wahr* [1990], and *Ponte et al.* [1991] agree that the IB effect fails for time periods less than a couple days but is a valid approximation for periods greater than a couple months. *Ponte et al.* used a numerical model to study the barotropic ocean response to observed pressure fields globally. *Wunsch* analyzed sea level records of Bermuda and came to the same conclusion on the timescale validity of the response.

Complications also arise due to the correlation of wind and surface pressure, which *Ponte et al.* avoided by using observed pressure fields from the U.S. National Meteorological Center (NMC) to isolate sea level changes due to pressure alone. Most studies have faced considerable problems with the high correlations. Other factors such as the size and shape of the basin also affect the IB behavior. *Wunsch and Stammer* [1997] go into detail beyond the scope of this study on the response due to various configurations of basins. They found that the inverted barometer response should be expected in deep water for most cases. Shallow water response is not well understood. *Ponte et al.* did not look at regions shallower than 1000 meters. *Wunsch and Stammer* [1997] discuss shallow water briefly referring to differing accounts in earlier work by *Robinson* [1964] and *Adams and Buchwald* [1969].

GPS stations IRKT, ALBH, and BAHR are all close to bodies of water. Their processed residual signals need to take atmospheric pressure loading as well as the IB effect into account in explaining periodic signals. BAHR is located on the Persian Gulf, a body of water 240,000 km^2 in area with a maximum depth of 90 meters. IRKT is near Lake Baikal in Siberia. It is the

deepest lake in the world reaching depths of nearly a mile spanning about 80 km in width and 636 km in length. Our model utilizes a global 1° by 1° grid of ocean-land distribution data to resolve bodies of water. Lake Baikal and the Persian Gulf are both treated as bodies subject to the IB response.

The definition of inland sites depends on the size of the pressure system. We can expect to see the IB response affecting inland displacements when the site is within the correlated distance of the center of the front. In theory we would see less vertical displacement at coastal sites than inland sites. ALBH and DRAO are two GPS stations in British Columbia. ALBH is near the coast and DRAO is farther inland. We expect to see an atmospheric signal at ALBH with a reduced magnitude in comparison to DRAO due to the IB response of the Pacific Ocean.

For an indication of the relative effect of the standard IB model, we will compare the results to output from a no IB model, in which water acts as a rigid lid to pressure change.

Meteorological Data

The atmospheric data sets used in this study to model the pressure loading effects are taken from an ftp site maintained by NOAA [*ftp.ncep.noaa.gov*]. This site provides real time data available for only twenty-four hours. It contains the one by one degree global analyses produced by the NCEP Global Data Assimilation System (GDAS) in six-hour increments. The files are in the /pub/fnl/ directory and are named gdas1.T**Z.PGrbFxx, where ** = 00, 06, 12, 18 are their analysis times and xx = 00, 06 are the forecast hours. All files are in GRIB (GRIdded Binary) format, the WMO (World Meteorological Organization) standard for gridded binary data exchange. An in depth description of the GRIB format can be found at the same ftp site under the /pub/nws/nmc/docs/gribed1/ directory.

There is a surface pressure field included in the files, which we do not use because it is unreliable and unsuitable for interpolation to GPS sites. Instead the surface pressure is found by inserting interpolated values of upper atmosphere temperature, geopotential height, and relative humidity in a hydrostatic pressure model.

GPS Data

We use GPS data downloaded from Scripps Orbit and Permanent Array Center (SOPAC, *http://sopac.ucsd.edu*) in the form of h-files from January 1999 to January 2002. H-files are daily solutions for positions and orbits with loose constraints [*Dong et al.*, 1998]. Using the standard 51 IGS (International GPS Service) reference stations, the Scripps h-files are analyzed in GLOBK with coordinate realization. GLOBK [*Herring,* 2000] creates the station position time series using atmospheric pressure, temperature and relative humidity values.

Water Load Data

We obtained water load data from the IERS (International Earth Rotation Service) Global Geophysical Fluids Center [*http://www.csr.utexas.edu/research/ggfc/dataresources.html*]. The data provides the water load for the upper 2 meters of soil with one-degree global spacing from the early 1990's to 1999.

Chapter 5

Atmospheric Pressure Loading and GPS Signals at Designated Sites

We look at four sites in detail to gain insight into loading phenomena. The sites were chosen based on their location, analysis history, annual scale changes, and the amount of data available. We concentrate on the effects on atmospheric pressure loading, hydrologic loading, differing analysis group results, and the standard inverted barometer model versus the rigid ocean model at these sites.

Designated Sites

ALBH and DRAO are two permanent GPS stations in British Columbia. ALBH (Albert Head, Victoria) is located near the Pacific Ocean while DRAO (Penticton) is approximately 450 km inland. There are two behaviors to examine at these sites: the relative influence of atmospheric pressure and surface water loading as well as the change in atmospheric pressure loading from ALBH to DRAO due to the inverted barometer effect. Since DRAO is located farther inland it is not as influenced by the oceans response to pressure as the ALBH site. We expect to see a larger atmospheric pressure loading contribution inland at DRAO.

IRKT (Irkutsk) is a station in Siberia located beside the deepest lake in the world, Lake Baikal. One interesting aspect of the IRKT data is the disagreement between analysis groups. We see changes in the agreement between groups over specific time intervals due to changes in analysis code. In comparing two groups GPS time series, the date at which the analysis code is altered in one is visible, usually as a vertical shift due to a change in acceptable elevation angle in the code. IRKT data in particular shows the alteration dates clearly. Of concern in this study is the agreement in annual periods independent of alterations in analysis code. If the annual period is a product of loading then all analysis codes should agree lest the signal is an artifact of processing. At IRKT we also are interested in comparing the standard inverted barometer models fit versus the rigid ocean models fit to the GPS data. Since Irkutsk is located in the middle of Asia, the only IB response should be due to Lake Baikal. The rigid lid ocean model should provide a larger loading signal. However, the standard IB model is expected to be a more accurate model of the atmospheric pressure contribution to loading. The difference between the two models should be relatively small due to a small, expected IB response of Lake Baikal. It is smaller than most pressure fronts and for that reason will be restricted in its response. For this

site, we also examine the atmospheric pressure contribution combined with surface water loading data to get a better idea of the total loading signal.

The final site we concentrate on is BAHR (Bahrain), a small country on the Persian Gulf. For BAHR we should see no snow loading, only groundwater and atmospheric pressure loading. Again, we are interested in the strength of the atmospheric pressure loading due to its proximity to a large body of water and the waters response to atmospheric pressure fluctuations.

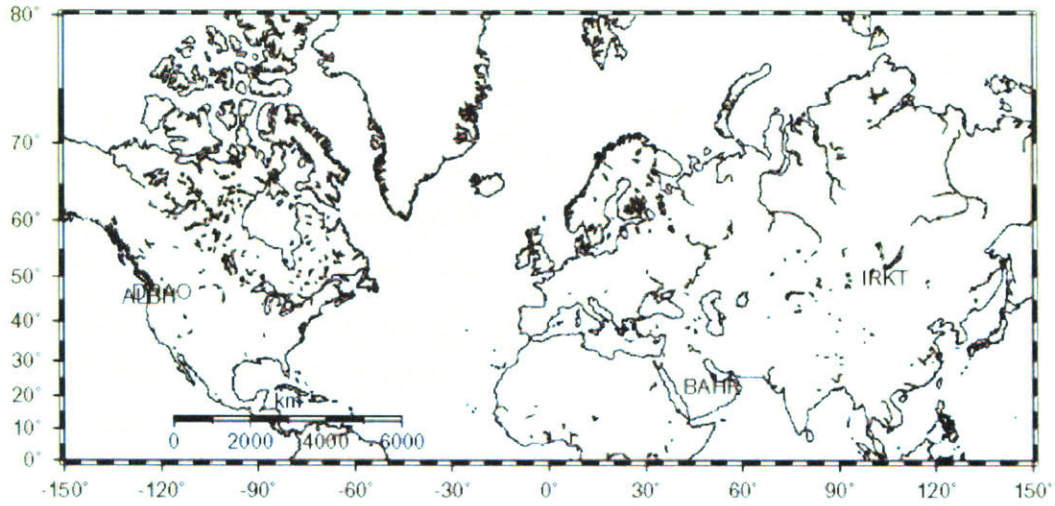

Fig 5.1 - Map of designated station locations

Site Analysis

The chosen sites, ALBH, DRAO, IRKT, and BAHR (See Fig. 5.1) are studied seeking a greater understanding of loading phenomena. To compare the GPS data (24 hour intervals) to the pressure loading data (6 hour intervals), we examined the mean-subtracted daily averages for both.

At Albert Head (ALBH) and Penticton (DRAO) we found a clear difference due to proximity to water. Figure 5.2 shows the GPS signal as well as the atmospheric pressure loading calculated using an inverted barometer (IB) response from the ocean, which will be referred to as standard pressure loading (as opposed to no IB or rigid lid pressure loading). Figure 5.3 displays both the standard atmospheric pressure loading and the no IB loading for both ALBH and DRAO. The loading signals at DRAO are virtually equal while at ALBH we see a spread in the standard and no IB values due to the relative proximities of the two sites to the Pacific Ocean.

The rms of the difference between the standard and no IB values at ALBH is approximately 1.8 mm, which is considerably larger than the rms value of approximately 1.1 mm at DRAO. Table 5.1 shows the closeness-of-fit findings as rms values for all four stations. As expected, for both ALBH and DRAO the standard atmospheric pressure loading model fits the GPS data better than the no IB model. You can see in the table that the

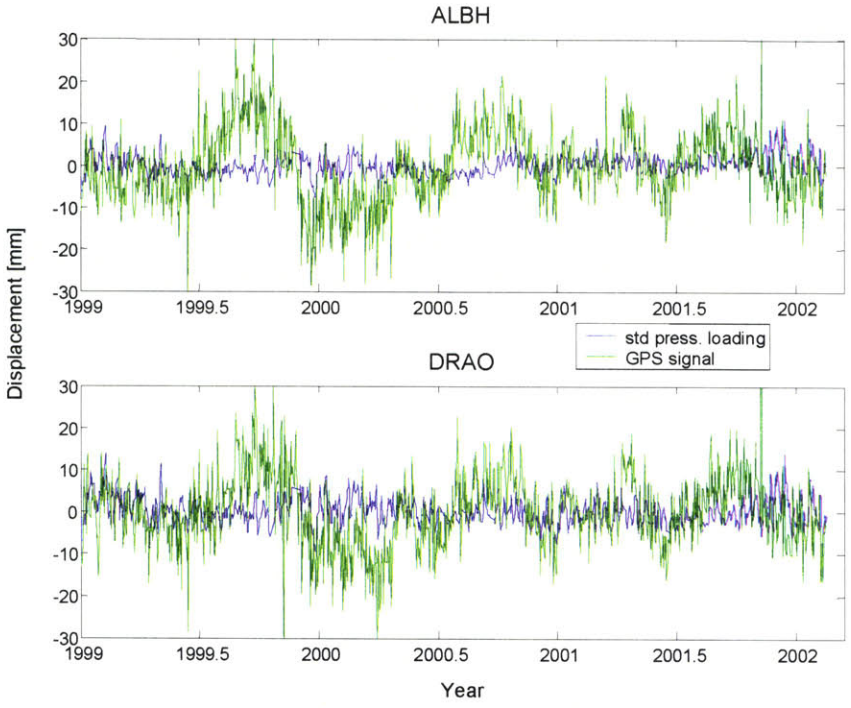

Fig 5.2 - GPS signal and standard atmospheric pressure load for ALBH and DRAO.

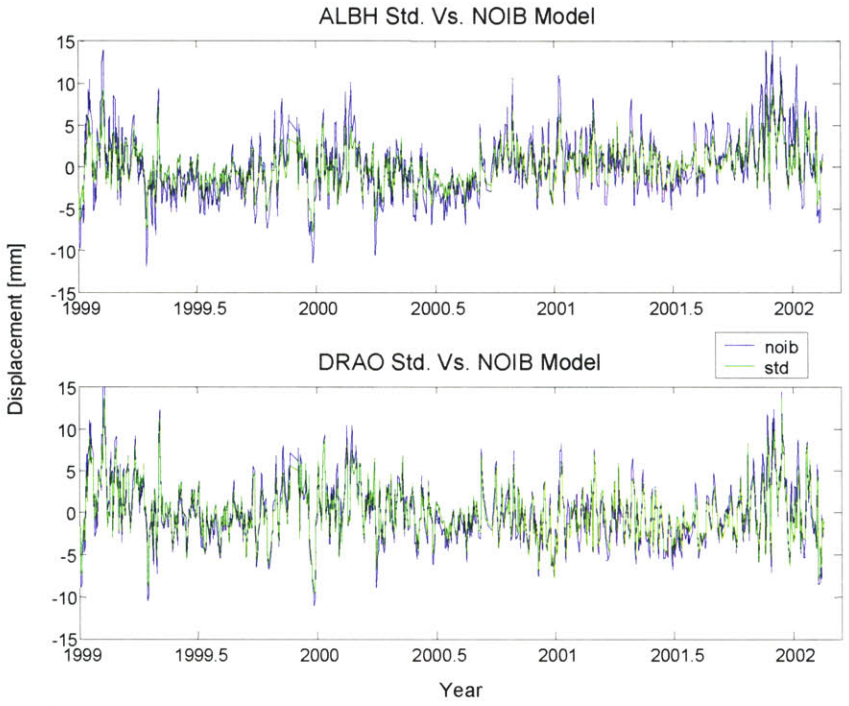

Fig 5.3 - Standard versus no IB models for ALBH and DRAO. There is a bigger difference between the two at ALBH because of its closer proximity to the ocean.

Site RMS Values [mm]

	GPS	IB	GPS-IB	100% Corr.	100% Uncorr.	dev from corr
ALBH	8.8	2.5	8.9	6.3	11.3	2.6
BAHR	12.6	3.0	10.9	9.6	15.6	1.3
DRAO	8.6	3.3	8.6	5.3	11.9	3.3
IRKT	11.9	4.5	9.9	7.4	16.4	2.5

	GPS	no IB	GPS-noIB	100% Corr.	100% Uncorr.	dev from corr
ALBH	8.8	3.8	9.3	5.0	12.6	4.3
BAHR	12.6	4.8	10.2	7.8	17.4	2.4
DRAO	8.6	3.8	8.6	4.8	12.4	3.8
IRKT	11.9	4.9	9.7	7.0	16.8	2.7

	IB-noIB
ALBH	1.8
BAHR	1.9
DRAO	1.1
IRKT	0.7

Table 5.1 - RMS values for the GPS data, standard IB pressure load, no IB pressure load, the difference between the GPS data and each of the pressure loads, and the deviation of the rms difference from the 100% correlated case for each site (in millimeters) as well as the rms of the difference between the IB and no IB models.

In Figure 5.2 the GPS signal is much stronger than the standard pressure loading. The atmospheric pressure loading signals, both standard and no IB, have amplitudes of less than 10 mm while the GPS signal has amplitudes closer to 20 mm. Other loading sources must be taken into account to explain the total loading signal expressed in the GPS signal. We have utilized water storage data from the IERS Global Geophysical Fluids Center to gain a broader understanding of the relative contributions of different loading sources. The data represents the amount of water in the upper 2 meters of soil. Figure 5.4 and 5.5 display the water storage data along with monthly averaged GPS measurements from 1993 to 1999 along with the 1999 to 2002 GPS daily averages and standard IB atmospheric pressure loading signal as well as monthly GPS data combining the two time periods. The water loads for ALBH and DRAO have amplitudes of approximately 10 mm with summer maxima and winter minima, although there is a larger water load at DRAO possibly due to snow. The atmospheric pressure load is in phase with the water load at both sites meaning that they have constructive interference and should add to provide a larger total loading contribution. We shifted the last few years of water loading data forward in time and in phase with the standard load and summed the two for a rough approximation of the combined load. Figure 5.6 displays the GPS signal and the resulting combined load. Table 5.2 gives rms values for the GPS data (also in Table 5.1), the combined load, and the difference between the two. Comparing these values with the ones in Table 5.1 we see a that the combined load is a better fit to the GPS signal than the atmospheric pressure load alone at ALBH and DRAO.

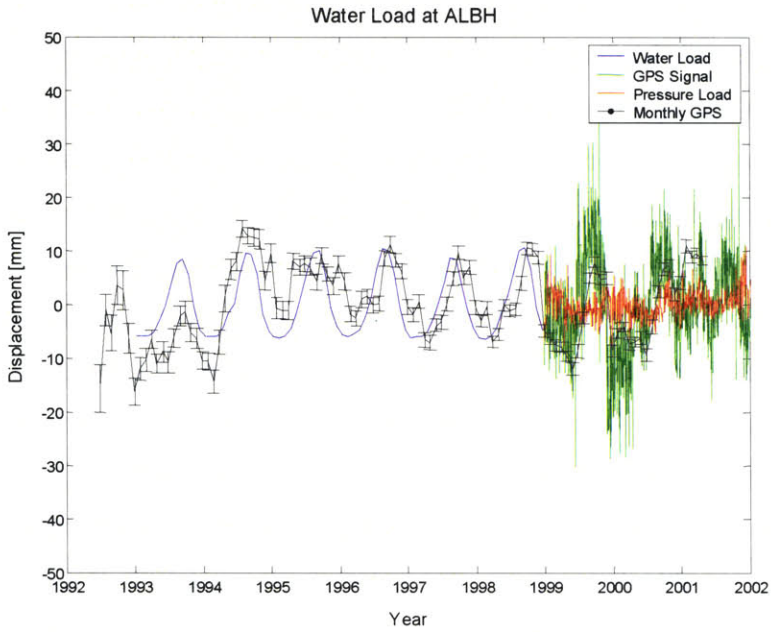

Figure 5.4 - Comparison of water load, GPS, and pressure load data at ALBH

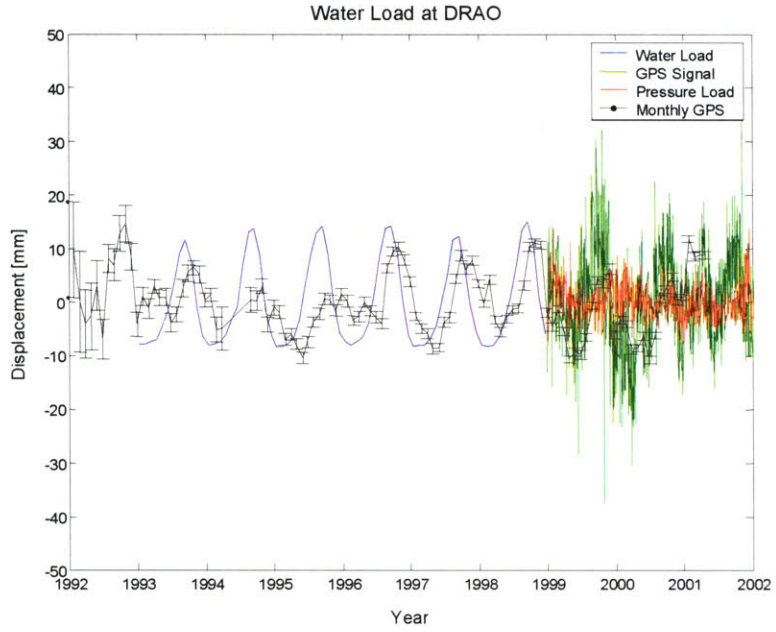

Figure 5.5 - Comparison of water load, GPS, and pressure load data at DRAO

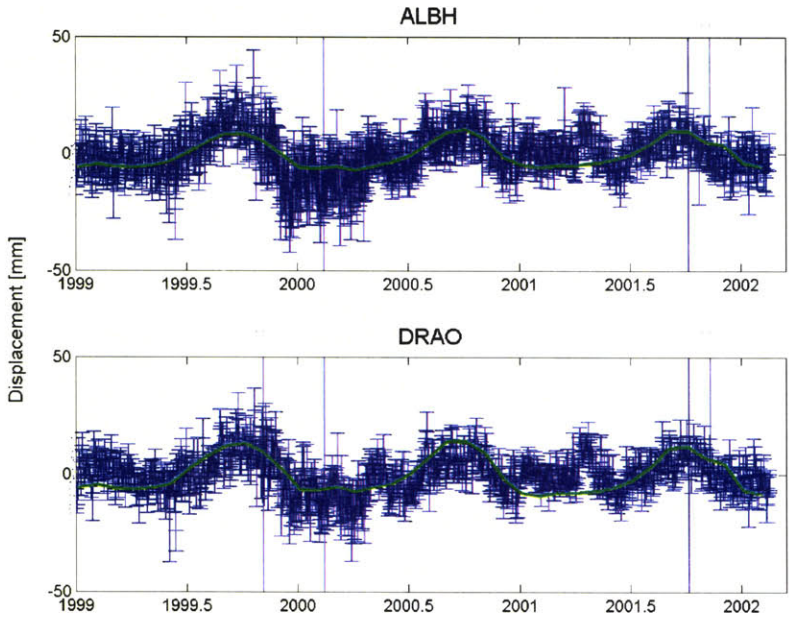

Fig 5.6 - GPS Signal for ALBH and DRAO along with the atmospheric pressure load plus the shifted water load.

	GPS [mm]	Tot [mm]	GPS-Tot [mm]
ALBH	8.8	5.7	6.0
BAHR	12.6	4.2	8.2
DRAO	8.6	7.7	8.0
IRKT	11.9	10.6	10.8

Table 5.2 - This table shows closeness of fit between the GPS data and the combined load. In comparing values to those in Table 5.1 we see better fits at ALBH, BAHR, and DRAO using the combined load instead of the atmospheric pressure load alone.

The GPS data from Irkutsk (IRKT) shows a strong annual signal (See Fig. 5.7). The standard pressure load is at about half of its amplitude. The pressure load model takes into account that IRKT is located on Lake Baikal, a body of water, which should respond as an inverted barometer to atmospheric pressure changes on seasonal and annual timescales [*Wunsch*, 1972]. The standard and no IB load are practically the same with a standard deviation of only approximately 0.7 mm (See Fig. 5.8). IRKT is so far inland that there is no IB response due to the ocean and the size of the lake is small compared to pressure fronts. Lake Baikal does not show a large IB response most likely because it is not large enough to accommodate the redistribution of water necessary due to the fact that it is smaller or around the same size as an average pressure front. As seen in Table 5.1, the no IB model has a smaller standard deviation

relative to the GPS signal than the standard load. However this closeness of fit comparison is not likely providing a reliable evaluation of the signals since both models are so close to one another.

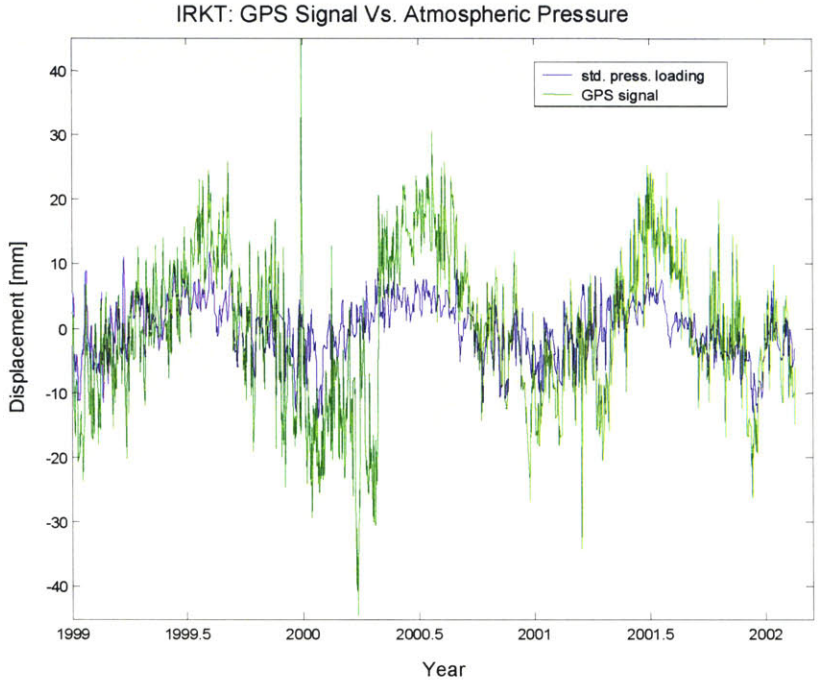

Fig 5.7 - GPS signal and atmospheric pressure load (standard IB model) for IRKT

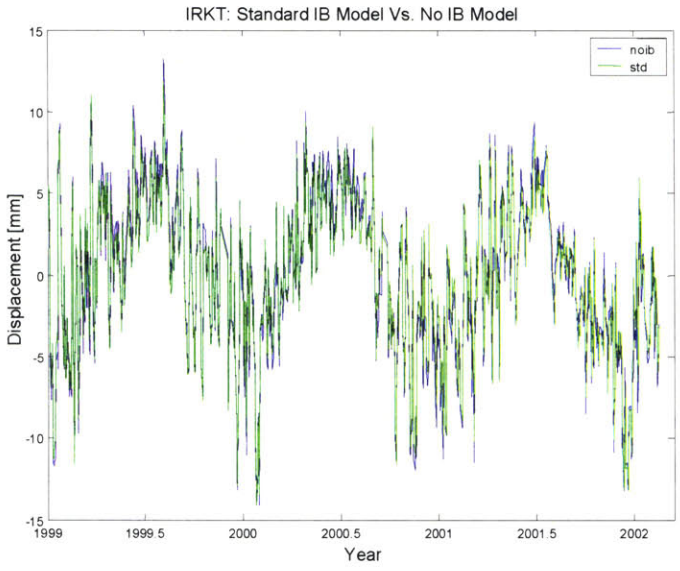

Fig 5.8 - Standard IB model and no IB model for IRKT.

The IERS water load data for IRKT is displayed in Figure 5.9. It looks roughly the same as the loads for ALBH and DRAO with amplitude of roughly 10 mm. It is also in phase with the

pressure load as well. This provides an explanation for the relative size of the GPS signal to the pressure load. The combined load is shown in Figure 10. The combined amplitude is roughly the same as the observed GPS signal. IRKT is the only site, which had a closer fit between the GPS data and the atmospheric pressure load than the GPS data and the combined load. However, we see a smaller deviation from the 100% correlated case when using the combined load. The combined load is a sum of the atmospheric pressure load and the water load from years before 1999. The water load from then may not be the same as it was when the GPS data was taken.

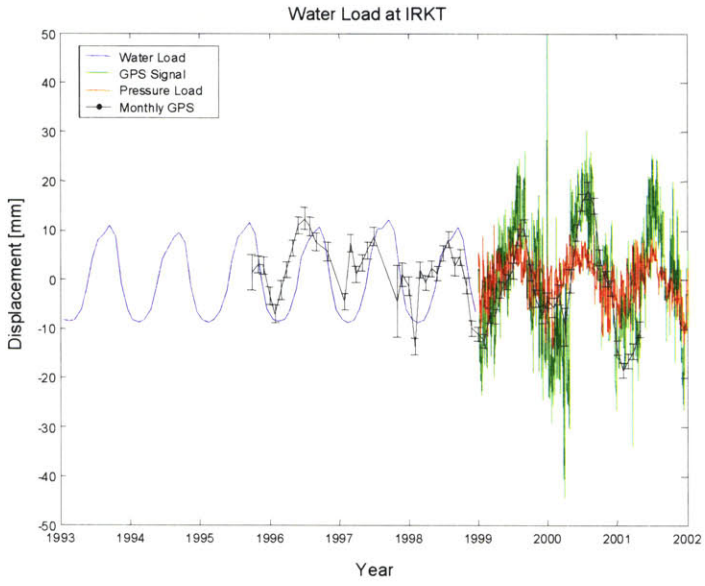

Figure 5.9 - Comparison of water load, GPS, and pressure load data at IRKT

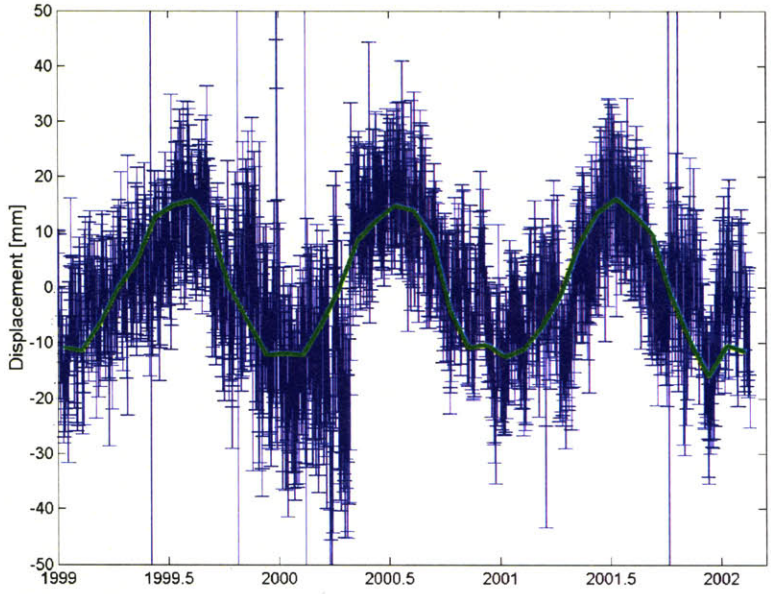

Fig 5.10 - This figure displays GPS data alongside the combined, atmospheric pressure load plus shifted water load for IRKT.

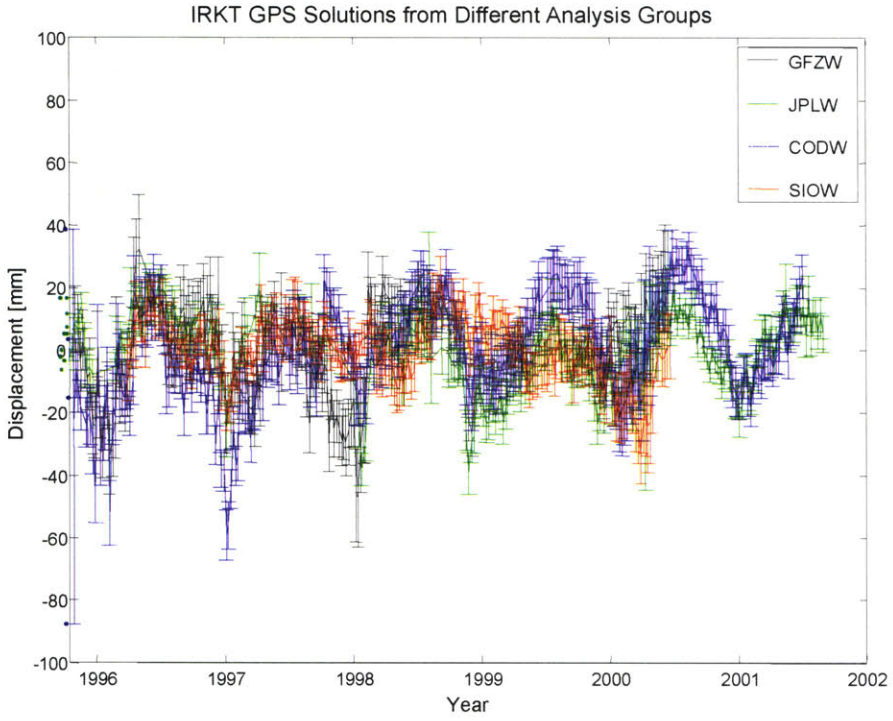

Figure 5.11 - IRKT global solutions from four different analysis groups.

Irkutsk GPS data in particular displays disagreements between analysis groups (See Fig 5.11). The disagreements generally take the form of abrupt vertical signal displacements due to a change in minimum elevation angle of data used in the analysis. The figure shows very close agreement between all of the analysis groups since 1999. We see a vertical shift in CODW around the end of 1997, JPLW around the start of 1999, and GFZW around the beginning of 1998. The amplitude and phases appear to stay the same during the alterations. Due to their consistency during change and their agreement with each other and loading factors, we have reason to believe that the signals are not simply artifacts of analysis complications.

BAHR is a permanent station on the Persian Gulf whose GPS signal lacks the added complication of snow loading. Figure 5.12 displays the atmospheric pressure load along with the GPS signal. The figure suggests that even if there is no snow loading, there are other factors adding to the annual surface displacements measured by GPS. The station is located on the Persian Gulf. Due to its close proximity to the gulf as well as the Arabian Sea, BAHR displays the largest difference between the standard and no IB pressure loads (See Fig 5.13) of all four sites. The no IB load actually fits the GPS data better than the standard load. The loads are very similar except the no IB load has the larger amplitude. Figure 5.14 shows the IERS water load data from 1993 to 1999 at Bahrain. The water and pressure load are in phase and if we assume the water load continues with the same period and amplitude through 2002, we can make a better estimate of the total loading contribution (See Fig. 5.15). The combined load has a larger amplitude that the standard atmospheric pressure load and accounts for the majority of the GPS signal observed. In Table 5.2 we see that the combined load fits the GPS data better than the atmospheric pressure load alone.

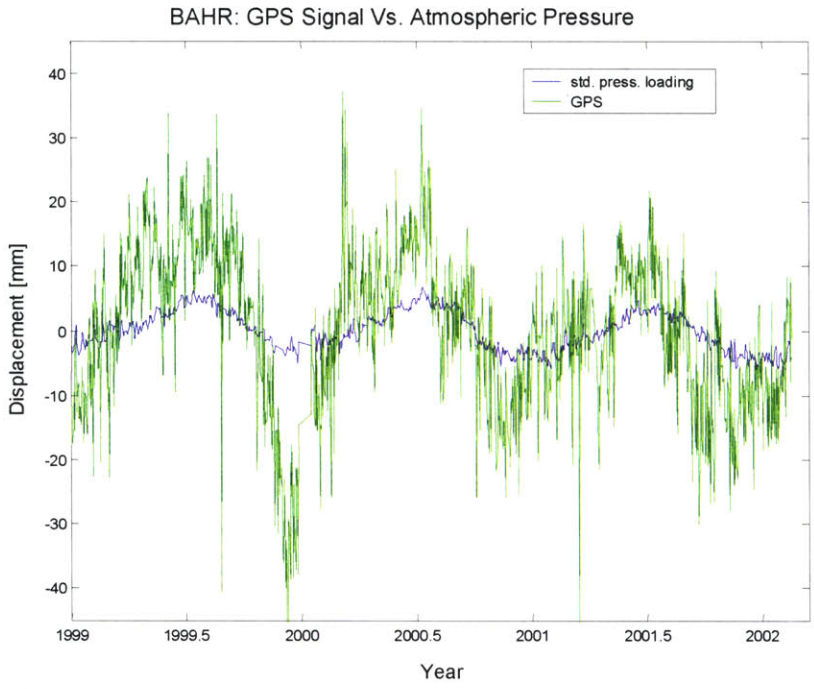

Fig 5.12 - GPS signal and Standard IB atmospheric pressure load for BAHR.

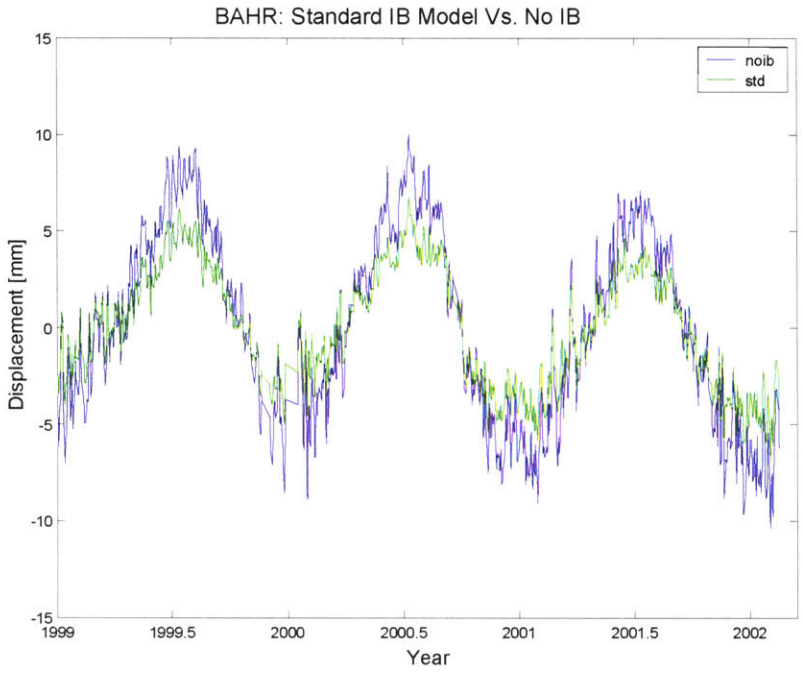

Fig 5.13 - Standard IB model and no IB model for BAHR.

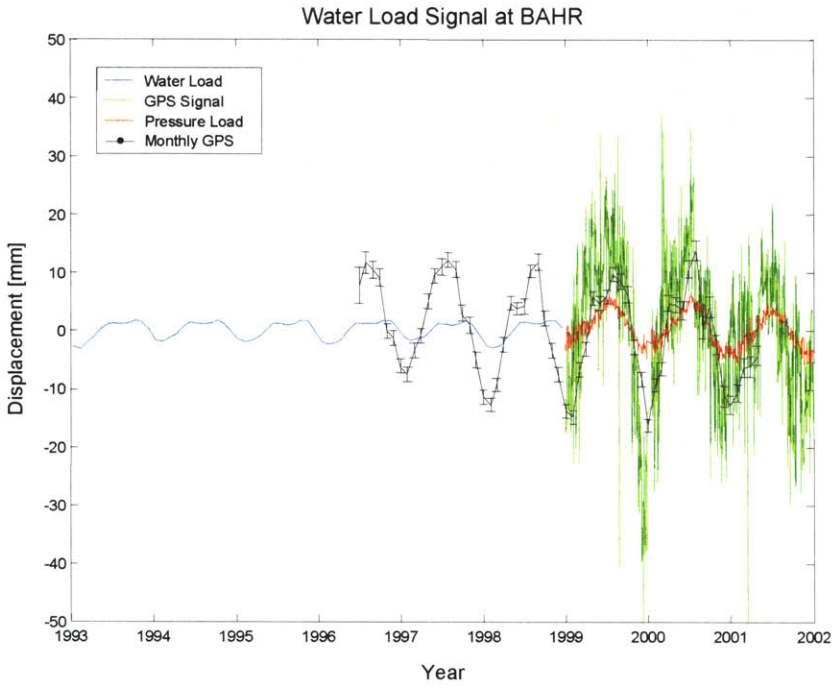

Figure 5.14 - Comparison of water load, GPS, and pressure load at BAHR

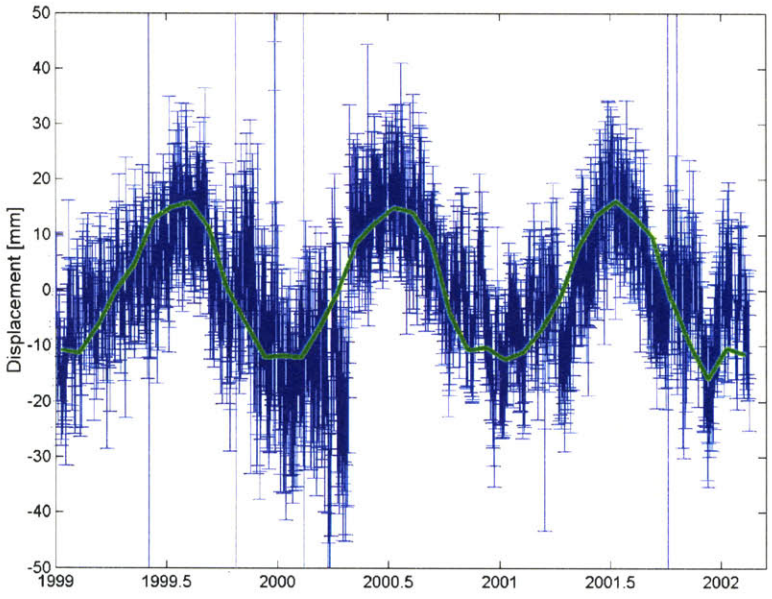

Fig 5.15 - Comparison of GPS signal to combined, atmospheric pressure load plus shifted water load for BAHR.

Further Analysis

To understand the nature of the GPS data and its relation to the pressure loads, we look at the winters and summers individually. Do the summers have an equal and opposite signal to the winter or are there separate winter and summer patterns? There is snow loading in some locations during winter months, seasonal fluctuations in groundwater, and smaller pressure variations during summer months so different patterns might be expected. We have analyzed the annual GPS pattern by taking the first winter's standard IB pressure loading data for each site and examining where it best fits the GPS data in time. Essentially we calculated the rms of the loading data to the GPS data as we shifted the first winter's loading data (from January 1999 to mid-March 1999) in time. The comparison utilized the winter mean-subtracted pressure loading data segment and the mean-subtracted GPS data. This "sliding rms" evaluation showed at better fit of the 1999 winter to other winters than to summers. All sites except BAHR had the lowest rms value (rms of difference between GPS data at different intervals and the first winter's standard pressure load) during the winter. Our results changed when we altered the number of sliding months. In other words, if we simply slide the January 1999 data we get different results. The best fits occurred sliding seasonal timescale chunks as seen here.

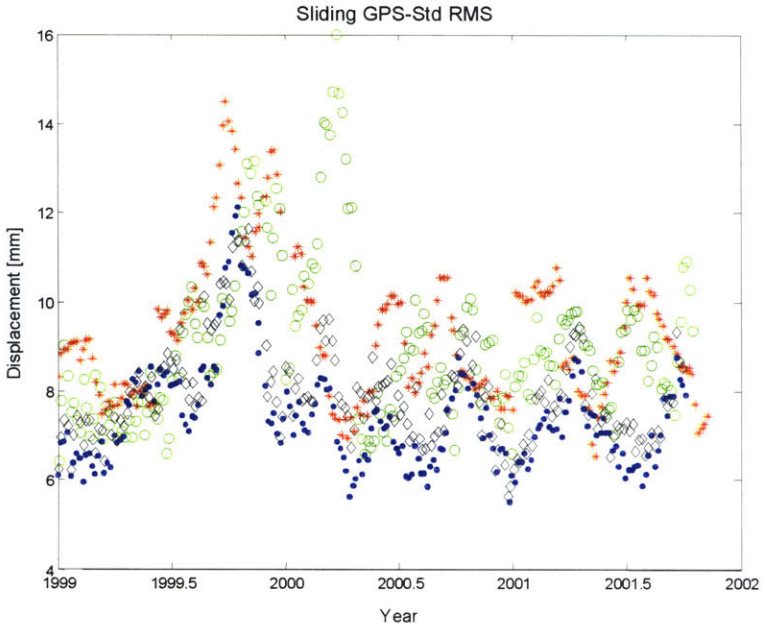

Fig 5.16 - Sliding RMS values of GPS-Std pressure load. Comparison of standard pressure load from winter 1999 with GPS data from 1999 to 2002. Cross represents BAHR, circle represents IRKT, dot represents ALBH, and diamond represents DRAO.

Upon further inspection, the atmospheric pressure loads fit the GPS data better during winter months than summer months at all four locations (See Table 5.3). Our atmospheric pressure loading model describes winter months better than summer months. This could be due to a number of reasons. Other seasonal scale fluctuations affecting radial positioning on the Earth could have a smaller influence during winter months, leaving atmospheric pressure loading with a larger contribution to the total seasonal displacement. However, we would not expect that at sites with a significant amount of snow loading in winter months, such as ALBH and DRAO. ALBH showed a significant improvement in fit during the winters while DRAO showed only a marginal improvement. In Siberia, at IRKT there is also a large reduction in the rms during the winter. The snow loading contribution is greater in these regions. Another explanation is that there is an even larger contributor to annual loading during the summer, leaving the pressure loading with more influence in the winter. A more detailed analysis of the relative impact of seasonal changes should be examined. However, such an undertaking is beyond the scope of this study. Another explanation for the better fits during the winters is that pressure variations are larger in the winter than the summer. We expect pressure loading to have a larger impact during these months. Pressure variations are also larger at high latitudes. Pressure loading signals tend to be larger at high latitudes during the winter than at lower latitudes during the summer simply because of the nature of the Earth's alignment with the Sun and its impact on the atmosphere. However, Table 5.3 give the rms values for summer and winter months and we see no noticeable increase from the summer to the winter pressure load rms values that we would expect for this explanation to be correct. The most likely explanation is one brought up by *Herring* [1990]. GPS position estimates could be noisier during the summer due to errors in estimating atmospheric delay. We do see this in our data as well. The rms values are systematically higher in the summer at each site.

Figure 5.17 shows a close up of the IRKT GPS data as well as the standard IB pressure load during winters of 1999, 2001, and 2002. Figure 5.18 displays close ups of the summers of 1999, 2000, and 2002 at IRKT. IRKT is a high-latitude location that displays the change of fit of pressure load to GPS between seasons visibly. The expected difference shown in Table 5.3 is the value for the rms of (GPS-Std) we would expect if the GPS and standard pressure load signals were 100% correlated. It is simply the difference between the GPS rms and the standard pressure load rms. The uncorrelated case is simply the sum of the GPS and pressure load rms

values. ALBH and DRAO show the lowest correlation between the GPS and pressure load signal.

Winter RMS [mm]

	GPS	Std	GPS-Std	Exp Diff	Uncorr.
ALBH	5.7	2.8	6.4	2.9	8.5
BAHR	10.0	3.0	9.1	7	13
DRAO	7.4	3.8	7.6	3.6	11.2
IRKT	11.5	4.8	8.9	6.7	16.3

Summer RMS [mm]

	GPS	Std	GPS-Std	Exp Diff	Uncorr.
ALBH	8.6	1.9	9.3	6.7	10.5
BAHR	12.7	3.8	10.4	8.9	16.5
DRAO	7.7	2.2	7.8	5.5	9.9
IRKT	14.3	4.3	11.0	10	18.6

Table 5.3 - Summer and winter RMS values (in millimeters) of GPS data, standard IB atmospheric pressure load, and the difference between the two. Winters and summers were calculated separately to see if the pressure load fit the GPS data better in the summer or in the winter. The expected difference column shows the RMS values we would expect for the difference if the load signal is quasi random and has no error, given the RMS for GPS and the standard pressure load.

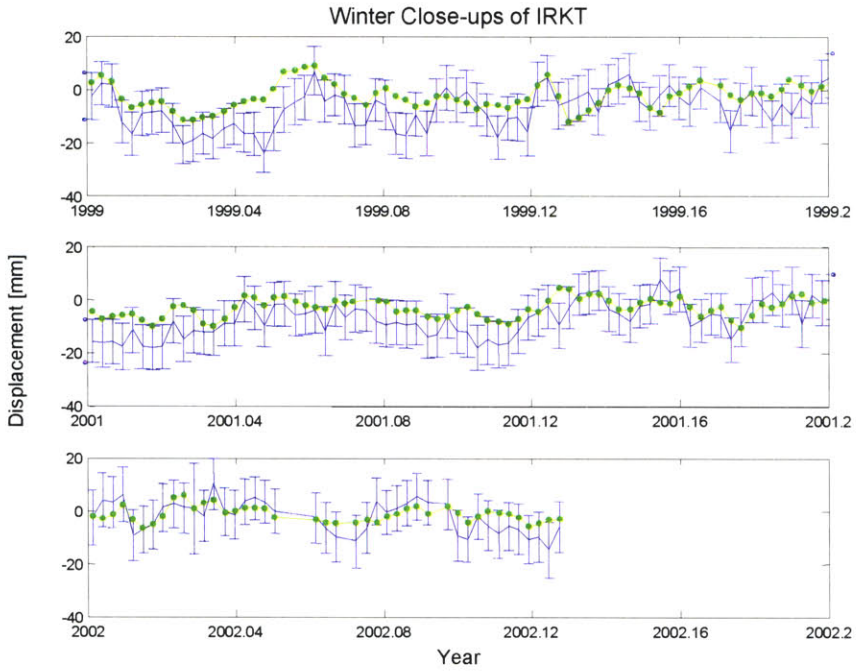

Fig 5.17 - Close-ups of IRKT winters. The green line is the standard model atmospheric pressure load and the blue is the GPS data. The two match very closely.

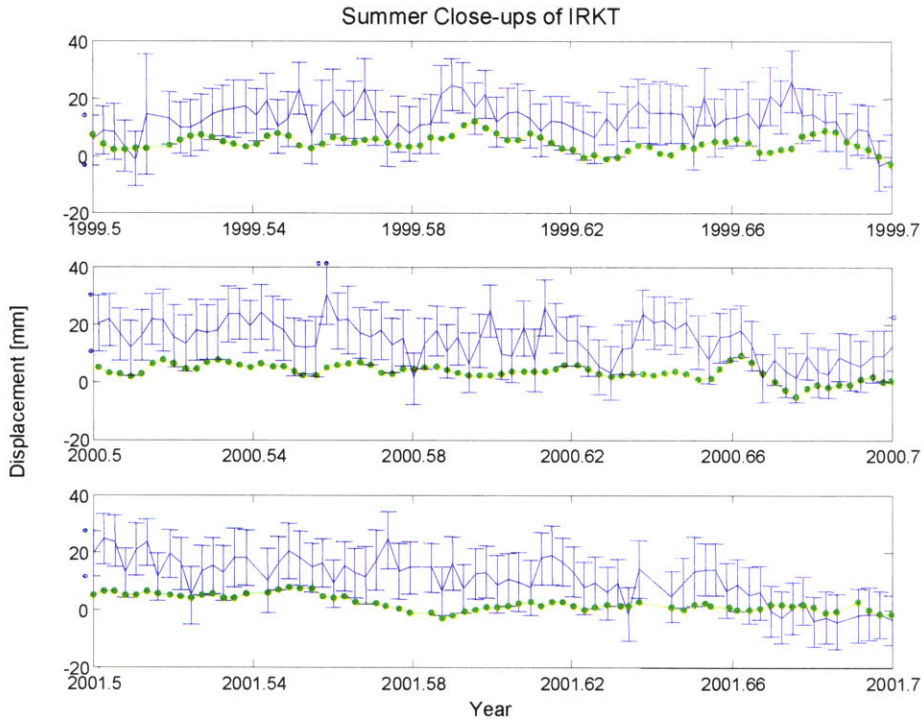

Fig. 5.18 - Summer close-ups of IRKT. The green line is the standard atmospheric pressure load and the blue is the GPS data. These two curves fit much better in the winter.

Chapter 6

Conclusions

GPS data from our four designated sites, ALBH, DRAO, BAHR, and IRKT has provided valuable information about our understanding of atmospheric pressure loading. Millimeter-level positioning capabilities allow for a realistic comparison of small pressure loads to actual measurements. This study has examined the contribution of atmospheric pressure loading to annual fluctuations in GPS height estimates. Focus has laid primarily on the inverted barometer effect, the relative impact of pressure loading in comparison to other sources of annual vertical displacements, and alternative sources of error, such as disagreements between analysis groups.

The inverted barometer response of large bodies of water, over time periods greater than a few days, to pressure changes has a noticeable effect on the atmospheric pressure load in coastal regions. Albert Head (ALBH) and Penticton (DRAO), a coastal and inland station pair located in British Columbia, Canada, show the influence of the inverted barometer effect with proximity to water. The standard inverted barometer pressure load at ALBH, the coastal site, fits the GPS data much better than the no IB load. At DRAO the standard pressure load only provides a small improvement over the no IB load to the GPS data. The no IB pressure loads fit the GPS data better than the standard load at Irkutsk (IRKT) and Bahrain (BAHR). However due to the fact that a quantification of all significant loading factors is beyond the scope of this study, the no IB pressure load fitting the GPS data the better only confirms what we already knew about our model although, BAHR suggests the no IB is better near restricted bodies of water. The no IB pressure load has a larger amplitude than the standard IB pressure load and therefore would naturally tend to provide a better fit to a signal with an even greater amplitude and equal periodicity.

Hydrologic loading sources have been quantitatively discussed here as an indicator of relative loading contributions. Water storage data from the IERS Global Geophysical Fluids Center has provided an approximate determination of the loading due to groundwater and snow loading. By shifting the water loads and adding them to the atmospheric pressure load we have seen a great improvement in the fit to the GPS data sets.

We found that the seasons have different signatures. Winter and summer signals are not simply opposites of each other since some of the different loading signatures, such as snow loading may appear for only one season. Analysis of the GPS data and standard pressure loads

shows a better fit between the two during winter months than during the summer. Pressure loading is a larger factor in the winter due to greater pressure fluctuations.

The agreement of the period of the GPS data and the model is great importance. At sites such as IRKT, changes in analysis methods by different analysis groups are visible and concern arises over the validity of a loading signal. How do we know the periodic signal is not an artifact of the processing? In examining the GPS data from IRKT for multiple groups, the processing alteration times stood out mainly as vertical displacements due mainly to changes in the acceptable antenna elevation angles. The periods remain unaffected.

Future

In the future more insight on loading phenomena could be gained by quantitatively examining measurements from significant loading sources together. Further studies should also include a quantitative analysis of all significant sources of loading, which is beyond the scope of this study. Also water below 2 meters depth should be accounted for. This would be especially helpful for long-term trends when we seeing gradual increases and decreases in the water table.

Significance

An understanding of atmospheric pressure loading provides a greater understanding of the dynamics of the Earth. Any measurements of the Earth's surface on timescales of days to years are affected by this phenomenon. Loading must be accounted for in precise geophysical measurements. Current geophysical studies actually use sites such as DRAO as references for regional solutions [*Dragert*, 2001] and are likely encountering effects due to atmospheric pressure loading, which we would like to account for.

References

Adams, J. K., and V. T. Buchwald, The generation of continental shelf waves, *J. Fluid Mech.*, 35, 815-816, 1969.

Blewitt, G., Advances in global positioning system technology for geodynamics investigations: 1978-1992, in *Contributions of Space Geodesy to Geodynamics: Technology, Geodyn. Ser.*, vol. 25, edited by D. E. Smith and D. L. Turcotte, pp. 195-213, AGU, Washington, D.C., 1993.

Dong, D. et al., Anatomy of apparent seasonal variations from GPS derived site position time series, publication pending

Dong, D., T. A. Herring, and R.W. King, Estimating regional deformation from a combination of space and terrestrial geodetic data, *J. Geodesy*, 72, 200-214, 1998.

Farrell, W. E., Deformation of the Earth by surface loads, *Rev of Geophys.*, 10, 761-797, 1972.

Gill, A. E., *Atmosphere-Ocean Dynamics,* 662 pp., Academic, San Diego, Calif., 1982.

Herring, T. A., J. L. Davis, and I. I. Shapiro, Geodesy by radio interferometry: The application of Kalman filtering to the analysis of VLBI data, *J. Geophys. Res.*, 95, 12561-12581, 1990.

Herring, T. A., Geodetic applications of GPS, *Proceedings of the IEEE*, 87, January 1, 1999.

Longman, I. M., A Green's function for determining the deformation of the earth under surface mass loads, 2, Computations and numerical results, *J. Geophys. Res., 68,* 485, 1963.

Manabe, S., T. Sato, S. Sakai, and K. Yokoyama, Atmospheric loading effect on VLBI observations, In proceedings of the AGU Chapman conference on geodetic VLBI: Monitoring global change, *NOAA Tech. Rep.,* NOS 137, NGS 49m 111-122, 1991.

Ponte, R. M., D. A. Salstein, and R. D. Rosen, Sea level response to pressure forcing in a barotropic numerical model, *J. Phys. Oceanogr.*, 21, 1043-1057, 1991.

Rabbel, W., and J. Zschau, Static deformations and gravity changes at the Earth's surface due to atmospheric loading, *J. Geophys.*, 56, 81-99, 1985.

Rabbel, W., and H. Schuh, The influence of atmospheric loading on VLBI-experiments, *J. Geophys.*, 59, 164-170, 1986.

Robinson, A. R., Continental shelf waves and the response of sea level to weather systems, *J. Geophys. Res.,* 69, 367-368, 1964.

Trupin, A., and J. Wahr, Spectroscopic analysis of global tide gauge sea level data, *Geophys. J. Int.,* 100, 441-453, 1990.

Wunsch, C., Bermuda sea level in relation to tides, weather, and baroclinic fluctuations, *Rev. Geophys.*, 10, 1-49, 1972.

Wunsch, C. and D. Stammer, Atmospheric loading and the oceanic "inverted barometer" effect, *Rev. Geophys.*, 35, 79-107, 1997.

van Dam, T. M., G. Blewitt and M. Heflin, Atmospheric pressure loading effects on Global Positioning System coordinate determinations, *J. Geophys. Res.*, 99, 23, 939-23, 950, 1994.

van Dam, T. M. and T. A. Herring, Detection of atmospheric pressure loading using very long baseline interferometry measurements. *J. Geophys. Res.*, 99, 4505-4517, 1994.

van Dam, T. M. and J. Wahr, Displacements of the Earth's surface due to atmospheric loading: effects on gravity and baseline measurements, *J. Geophys. Res.,* 92, 1282-1286, 1987.

van Dam, T. M. and J. Wahr, Modeling environmental loading effects: a review. *Phys. Chem. Earth*, 23, 1077-1087, 1998.

-2478-16